



## Performance Evaluation of Nanofluid ( $\text{Al}_2\text{O}_3/\text{H}_2\text{O}-\text{C}_2\text{H}_6\text{O}_2$ ) Based Parabolic Solar Collector Using Both Experimental and CFD Techniques

K. Ajay\*, L. Kundan

Mechanical Engineering Department, Thapar University, India

### PAPER INFO

#### Paper history:

Received 04 December 2015

Received in revised form 20 February 2016

Accepted 14 April 2016

#### Keywords:

Solar Energy

Parabolic Solar Collector

CFD

Nanofluid

Thermal Efficiency

### ABSTRACT

The present work evaluates the performance of solar collector using  $\text{Al}_2\text{O}_3-\text{C}_2\text{H}_6\text{O}_2-\text{H}_2\text{O}$  nanofluid as a working fluid through both experimental and CFD analysis. Ethylene-glycol water mixture (40:60 v/v) is used as base fluid, where  $\alpha-\text{Al}_2\text{O}_3$  nanoparticle of 20 nm average size is dispersed for the preparation of nanofluid of four different volumetric concentration (vol. conc.) of 0.05, 0.075, 0.1 and 0.125%. Three different volume flow rates of 30 LPH, 50 LPH and 80 LPH are used. CFD analysis is carried out through ANSYS FLUENT 14.5. From both experimental and CFD analysis, an improvement in overall efficiency of solar collector is reported when nanofluid is used as compared to water-ethylene glycol mixture. With 0.125% vol. conc. of nanofluid  $\text{Al}_2\text{O}_3-\text{C}_2\text{H}_6\text{O}_2-\text{H}_2\text{O}$  (DI) maximum overall efficiency of about 4.6, 7.9 and 14.8% is reported at 30 LPH, 50 LPH and 80 LPH, respectively from CFD results while from experimental results maximum overall efficiency of about 4.3, 7.5 and 13.8% is seen at 30 LPH, 50 LPH and 80 LPH, respectively. Also, with increasing volume flow rate of working fluid, corresponding improvement in the overall efficiency of solar collector takes place. Close agreement is also developed between experimental and CFD result.

doi: 10.5829/idosi.ije.2016.29.04a.17

## 1. INTRODUCTION

Solar energy is one of the effective renewable energy available for us. Earth surface is incident by huge amount of solar radiations, about 174 PW of solar energy in a year [1]. Solar collectors are those types of devices which are used to transform the solar energy to useful form as heat to the working fluid flowing within the absorber tube of the solar collector [2]. Parabolic solar collectors are basically concentrating type of solar collectors, where solar flux is made to concentrate over the absorber tube of the collector [3]. Lower efficiency of such collector due to normal and conventional working fluids having poor thermo-physical properties has created a greater problem [4]. So, need for modifying the thermal properties of such working fluids has become major need in order to meet the increasing demand of energy [5]. Nanofluid, being an innovative

fluid has been used to resolve the heat transfer related problems due to its improved thermo-physical properties [6].

Various different types of nanofluids having different base fluids like water, ethylene glycol and therminol VP-1 and having different nanomaterials consisting of gold, silver, copper, aluminium and their corresponding oxides has been used as working fluids for the solar collectors [7]. Nanofluids have got remarkable features as they enhance the system efficiency due to their better thermal properties like better thermal conductivity and heat transfer coefficient [8] and also they directly absorb the incident solar radiation, thereby avoiding intermediate stage of heat transfer and so, associated heat losses are avoided [9]. Recently, various researches have taken place with usage of nanofluid as main working fluid in solar collector. Tyagi et al. [10] conducted a theoretical investigation of flat plate solar collector using  $\text{Al}-\text{H}_2\text{O}$  nanofluid. They have found that, an improvement of about 10% in the efficiency of solar collector takes

\*Corresponding Author's Email: ketan.bhardwaj88@gmail.com (K. Ajay)

place when water is replaced by Al-H<sub>2</sub>O nanofluid. Otanicar et al. [11] performed an experimental analysis of thermal properties of various different nanofluids made from different nanomaterials like carbon nanotubes, graphite and silver. They have concluded that an improvement of 5% in the efficiency of solar collector takes place when nanofluid is used as compared to water.

Chougule et al. [12] carried out an experimental analysis to study the effect of using nanofluid as working fluid in a solar water heater. Six different volume fractions of nanofluid were taken (0.2, 0.4, 0.6, 0.8, 1.0 and 1.2). It was concluded that the measured thermal conductivity of nanofluid enhanced with an increase in volume concentration of nanofluid. Hanet al. [13] performed an experimental analysis in order to evaluate the thermo-physical and optical properties of carbon black aqueous nanofluid to be used as working fluid in the solar collector. Four different volume concentrations of the nanofluid were taken as 4.4, 5.5, 6.6 and 7.7%. It was revealed that enhancement in the photo-thermal properties were seen at high volume concentration. Chaji et al. [14] carried out an experiment in order to evaluate the thermal efficiency of flat plate solar collector using TiO<sub>2</sub>-H<sub>2</sub>O nanofluid in flat plate solar collector (FPSC). Nanofluid at three different mass flow rates of 36 liter per hour, 72 liters per hour and 108 liters per hour were used. Three different volumetric concentrations of the nanofluid (without surfactant) i.e. 0.1, 0.2 and 0.3% were used. From the conducted experimental research it was found out that with an increment in the mass flow rate of the working fluid an improvement in the collector efficiency was seen which accounts to value of 15.7%. Alim et al. [15] evaluated both entropy generation and the pressure drop for nanofluid based flat plate solar collector. Different oxide nanoparticles (Al<sub>2</sub>O<sub>3</sub>, TiO<sub>2</sub>, SiO<sub>2</sub>, CuO) were made to disperse into the water, for the formation of the desired nanofluid to be used as a working fluid in flat plate solar collector. Nanofluid of different volume fractions ranging from 1-4% was made to flow with a different mass flow rates ranging from 1-4 liters per min, within the collector tube. From the conducted research, it was concluded that there was reduction in entropy generation and enhancement of heat transfer coefficient of 4.34 and 22.5% takes place respectively with CuO-H<sub>2</sub>O nanofluid as working fluid. Saini et al. [4] have found out that when nanofluid of carbon nanohorns in water is used, improvement in both thermal efficiency and instantaneous efficiency is seen as compared to conventional working fluid of water.

## 2. EXPERIMENTAL METHODOLOGY

### 2. 1. Description About Experimental Set Up

Schematic of experimental analysis is shown in Figure

1. Specification of the parabolic solar collector is shown in Table 1. Main components of parabolic concentrating solar collector includes:

- Absorber tube
- Reflector
- Storage tank
- Insulating piping arrangement
- Pump
- Flow regulating valve

Experiment is carried with five different working fluids including water-ethylene glycol mixture (60:40v/v), nanofluid of 0.05% vol. conc. Al<sub>2</sub>O<sub>3</sub>- C<sub>2</sub>H<sub>6</sub>O<sub>2</sub>-H<sub>2</sub>O (DI) (40:60 v/v), 0.075% vol. conc. Al<sub>2</sub>O<sub>3</sub>-C<sub>2</sub>H<sub>6</sub>O<sub>2</sub>-H<sub>2</sub>O (DI) (60:40 v/v), 0.1% vol. conc. Al<sub>2</sub>O<sub>3</sub>- C<sub>2</sub>H<sub>6</sub>O<sub>2</sub>-H<sub>2</sub>O (DI) (40:60 v/v) and 0.125% vol. conc. Al<sub>2</sub>O<sub>3</sub>- C<sub>2</sub>H<sub>6</sub>O<sub>2</sub>-H<sub>2</sub>O (DI) (40:60 v/v), where working fluid is made to flow at three different volume flow rates of 30 LPH, 50 LPH and 80 LPH.

**2. 2. Working Procedure** Working fluid (7 liters quantity) namely water-ethylene glycol mixture (60:40 v/v), nanofluid of 0.05% vol. conc. Al<sub>2</sub>O<sub>3</sub>- C<sub>2</sub>H<sub>6</sub>O<sub>2</sub>-H<sub>2</sub>O (DI) (40:60 v/v), 0.075% vol. conc. Al<sub>2</sub>O<sub>3</sub>-C<sub>2</sub>H<sub>6</sub>O<sub>2</sub>-H<sub>2</sub>O (DI) (60:40 v/v), 0.1% vol. conc. Al<sub>2</sub>O<sub>3</sub>- C<sub>2</sub>H<sub>6</sub>O<sub>2</sub>-H<sub>2</sub>O (DI) (40:60 v/v) and 0.125% vol. conc. Al<sub>2</sub>O<sub>3</sub>- C<sub>2</sub>H<sub>6</sub>O<sub>2</sub>-H<sub>2</sub>O (DI) (40:60 v/v) is made to circulate inside the absorber tube from the storage tank at three different working flow rates of 30 LPH, 50LPH and 80 LPH through the insulating piping arrangement.

In the absorber tube, working fluid picks up the incident solar energy, which is directly falling over the absorber tube and solar energy which is made to Reflector is basically of a parabolic shaped, having a mirror strips. Storage tank is made insulated, through insulating sheets and glass wool in-order to avoid any kind of heat loss. Readings of both inlet and outlet temperatures is taken through thermometer, which are placed at inlet and outlet sections of the absorber tube. Solar energy is measured through solar power meter, while wind velocity is measured through anemometer. All, the recordings are taken from 9.30 am to 2.30 pm, with an interval period of 30 minutes.

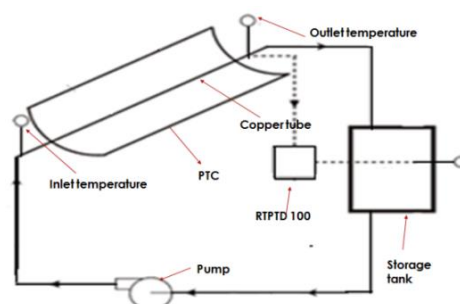


Figure 1. Schematic of experimental set up

**TABLE 1.** Specifications of parabolic shaped concentrating solar collector

Parameter	Value
Collector length, L	1.20 m
Collector breadth, W	0.915 m
End plate thickness	2 mm
Aperture area, $A_{\text{apper}}$	1.0188 m <sup>3</sup>
Rim angle	90 degrees
Focal length	0.30 m
Receiver inside diameter (D <sub>i</sub> )	0.027 m
Receiver outside diameter (D <sub>o</sub> )	0.028m
Receiver length	1000 mm
Glass envelope inside diameter, (D <sub>ei</sub> )	0.064 m
Glass envelope outside diameter, (D <sub>eo</sub> )	0.066 m
Insulation on pipes	Aluminum foil, superlon
Concentration ratio, C <sub>r</sub>	9.66

**2. 3. Preparation of Nanofluid** Al<sub>2</sub>O<sub>3</sub>-C<sub>2</sub>H<sub>6</sub>O<sub>2</sub>-H<sub>2</sub>O (DI) (60:40 v/v) nanofluid, of various different volumetric concentrations is prepared through two step methods. Firstly, known amount of α-Al<sub>2</sub>O<sub>3</sub> nanoparticle of 20 nm average size is made to disperse in the base fluid of C<sub>2</sub>H<sub>6</sub>O<sub>2</sub>-H<sub>2</sub>O (DI) (60:40 v/v). TEM image of the used α-Al<sub>2</sub>O<sub>3</sub> nanoparticle is shown in Figure 2. Amount of nanoparticle required for the preparation of nanofluid of desired vol. conc. is shown in Table 2.

After dispersion of nanoparticles in a base fluid of H<sub>2</sub>O-C<sub>2</sub>H<sub>6</sub>O<sub>2</sub> (60:40 v/v), mixing of this prepared sample takes place in a magnetic stirrer where through magnetic action nanoparticles are made to disperse properly. After this, sample formed is then placed in an ultrasonicator where nanoparticles are broken, so that nanofluid having finely suspended nanoparticle is prepared which is ready to be used as a working fluid.

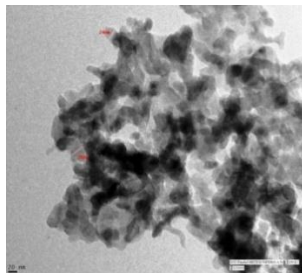


**Figure 2.** TEM image of α-Al<sub>2</sub>O<sub>3</sub> nanoparticle

**TABLE 2.** required amount of nanoparticle (grams)

Volumetric concentration %	Weight of nanoparticles (grams.) for 1 liter
0.050	1.985
0.075	2.977
0.100	3.970
0.125	4.962

Figure 3 shows the different sample of water-ethylene glycol and Alumina-water-ethylene glycol based nanofluid of different vol. conc. to be used as heat transfer medium in solar collector.

**2. 4. Governing Mathematical Model for Thermo-Physical Properties of Nanofluid**

Various thermophysical properties of nanofluid is calculated through following different models:

1. Density of nanofluid

$$\rho_{nf} = f_v \rho_{np} + (1 - f_v) \rho_{bf} \tag{1}$$

where,  $\rho_{np}$ ,  $\rho_{nf}$ ,  $\rho_{bf}$ , are the density of nanoparticle (kg/m<sup>3</sup>), density of nanofluid (kg/m<sup>3</sup>), density of base fluid (kg/m<sup>3</sup>) respectively and  $f_v$  is the volume concentration of nanofluid.

2. Specific heat of nanofluid

$$C_{nf} = \frac{f_v \rho_{np} C_{np} + (1 - f_v) \rho_{bf} C_{bf}}{\rho_{nf}} \tag{2}$$

where:  $C_{nf}$ ,  $C_{np}$ ,  $C_{bf}$  are the specific heat of the nanofluid, nanoparticle and base fluid respectively in J/kg-K.

3. Thermal conductivity of nanofluid

$$K_{nf} = \left[ \frac{K_{np} + 2K_{bf} + 2f_v(K_{np} - K_{bf})}{K_{np} + 2K_{bf} - f_v(K_{np} - K_{bf})} \right] K_{bf} \tag{3}$$

where:  $K_{nf}$ ,  $K_{bf}$ ,  $K_{np}$  are the thermal conductivity of the nanofluid, base fluid and nanofluid respectively in the W/m-K.

4. Dynamic viscosity of nanofluid

$$\mu_{nf} = \frac{\mu_{bf}}{(1 - f_v)^{2.5}} \tag{4}$$

where:  $\mu_{nf}$ ,  $\mu_{bf}$  are the dynamic viscosity of the nanofluid and base fluid respectively.

**3. CFD METHODOLOGY**

CFD analysis of absorber tube of a parabolic concentrating solar collector is done through ANSYS FLUENT 14.5.

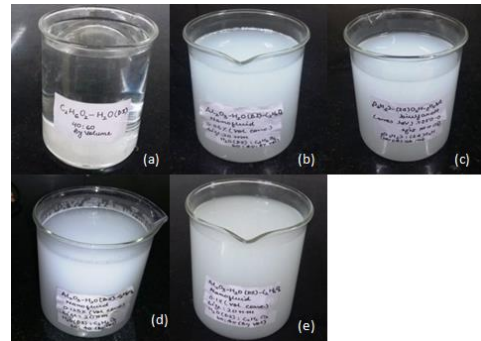


**Figure 3.** Various different prepared sample used as a working fluid (a) water-ethylene glycol mixture, (b) 0.05% vol. conc. Al<sub>2</sub>O<sub>3</sub>-C<sub>2</sub>H<sub>6</sub>O<sub>2</sub>H<sub>2</sub>O, (c) 0.075% vol. conc. Al<sub>2</sub>O<sub>3</sub>-C<sub>2</sub>H<sub>6</sub>O<sub>2</sub>H<sub>2</sub>O, (d) 0.1% vol. conc. Al<sub>2</sub>O<sub>3</sub>-C<sub>2</sub>H<sub>6</sub>O<sub>2</sub>H<sub>2</sub>O, (e) 0.125% vol. conc. Al<sub>2</sub>O<sub>3</sub>-C<sub>2</sub>H<sub>6</sub>O<sub>2</sub>H<sub>2</sub>O

Modelling of nanofluid is carried through one phase modelling technique available with the code of CFD. Modelling of solar fluxes is done through both solar load cell and solar ray tracing. Various different methodologies adopted for carrying out CFD analysis of absorber tube of a parabolic solar collector are depicted below.

**3. 1. Geometric Modelling** First of all, geometric model of the absorber tube is created using design modeller software available within the ANSYS as shown in Figure 4. Absorber tube basically consists of two concentric tube, one tube is for the fluid domain region while, other is basically for the glass covering.

**3. 2. Meshing of Geometric Model** Meshing of the geometric model is used for discretisation of the absorber tube. In the conducted analysis, hexahedral mesh is used. Meshed model of the absorber tube is shown in Figure 5.

**3. 3. Physical Modelling** For carrying out CFD simulation of the absorber tube, various different physical models are applied such as:

- Flow behaviour model
- Energy model
- Solar load model
- Radiation model (S2S radiation model)

**3. 3. 1. Flow Behaviour Model** In this type of physical model, the flow behaviour of the fluid flowing within the absorber tube is specified. After evaluating the Reynolds for all different working fluid, it is found that the Reynolds is greater than 4000. So, turbulent modeling schemes is used. In turbulent modelling schemes K-ε turbulent model is used.

**3. 3. 2. Energy Model** This model is generally used for study the heat transfer from the working fluid flowing in the absorber tube.

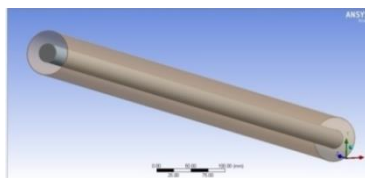


Figure 4. Geometry model of HCE (absorber tube)

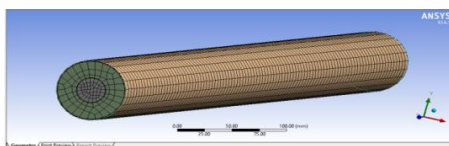


Figure 5. Meshed model of HCE (absorber tube)

**3. 3. 3. Solar Load Model** Solar load model is generally applied for modelling the solar fluxes. In solar load cell, various inputs such as latitude and longitude of location, day and time of the analysis and mesh orientation have been applied. On substitution of various inputs, we obtain the values of direct and diffuse solar radiations and vector of sun direction are obtained.

**3. 3. 4. Radiation Model** S2S (surface to surface) type of radiation model is used for modelling the radiation heat transfer, which is taking place in the system. In S2S model, various view factors of the concerned involved zones of the absorber tube is also calculated.

**3. 4. Physical Properties of the Concerned Working Fluid** The nature and physical properties of the working fluid is applied under this scheme available within the ANSYS FLUENT. Various thermo-physical properties of the used working fluid and material associated with HCE is shown in Table 3

**3. 5. CFD Governing Equations** In order the simulate the absorber tube of the solar collector, so as to obtain the temperature contours with different working fluids at different flow rate, various governing equation of mass, momentum and energy are to be solved, which are depicted below:

(a) Continuity equation

$$\frac{\partial \rho}{\partial t} + \frac{\partial(\rho u_j)}{\partial x_i} = 0 \quad (5)$$

(b) Momentum equation

$$\frac{\partial(\rho u_i)}{\partial t} + \frac{\partial(\rho u_i \rho u_j)}{\partial x_i} = \frac{\partial}{\partial x_j} \left[ \rho \delta_{ij} + \mu \left( \frac{\partial u_i}{\partial x_j} + \frac{\partial u_j}{\partial x_i} \right) \right] + \rho g_i \quad (6)$$

(c) Energy equation

$$\frac{\partial(\rho c_p T)}{\partial t} + \frac{\partial(\rho u_i c_p T)}{\partial x_i} - \frac{\partial}{\partial x_j} \left[ \lambda \frac{\partial T}{\partial x_j} \right] = S_T \quad (7)$$

(d) Turbulence Kinetic energy equation

$$\frac{\partial(\rho k)}{\partial t} + \frac{\partial(\rho k u_i)}{\partial x_i} = \frac{\partial y \left[ \Gamma_k \frac{\partial k}{\partial x_j} \right]}{\partial x_j} + G_k - Y_k + S_k \quad (8)$$

where,  $u_i$  is time averaged velocity vector,  $\rho$ ,  $c_p$ ,  $T$ ,  $k$  are density, specific heat, temperature and thermal conductivity of the working fluid, respectively.  $\delta_{ij}$ ,  $G_k$  and  $\lambda$  are kronecker delta function, generation of turbulence KE due to mean velocity gradients and bulk viscosity coefficient, respectively.  $x_i$  and  $x_j$  are spatial coordinate,  $\mu_t$  is eddy viscosity and  $\Gamma_k = (\mu_t/\sigma_k)$  and  $S_k$  is transport of KE due to diffusion.

**3. 6. Boundary Conditions** Various different boundary conditions, applied to solve the different governing equation is shown in Table 4.

**TABLE 3.** various Thermo-physical properties of materials and working fluids associated with HCE

Material/working fluid	Density ( $\rho$ ) kg/m <sup>3</sup>	Specific heat ( $C_p$ ) J/kg-K	Thermal conductivity (K) W/m-K	Dynamic viscosity ( $\mu$ ) Pa-s
H <sub>2</sub> O-C <sub>2</sub> H <sub>6</sub> O <sub>2</sub> (60:40 by vol.)	1057	3970	0.42	1.59e-3
0.05% Al <sub>2</sub> O <sub>3</sub> - H <sub>2</sub> O- C <sub>2</sub> H <sub>6</sub> O <sub>2</sub>	1179.85	3103.625	0.546	1.148e-3
0.075% Al <sub>2</sub> O <sub>3</sub> - H <sub>2</sub> O- C <sub>2</sub> H <sub>6</sub> O <sub>2</sub>	1253.75	3025.582	0.585	1.227e-3
0.1% Al <sub>2</sub> O <sub>3</sub> - H <sub>2</sub> O- C <sub>2</sub> H <sub>6</sub> O <sub>2</sub>	1326.7	2842.75	0.625	1.314e-3
0.125% % Al <sub>2</sub> O <sub>3</sub> - H <sub>2</sub> O- C <sub>2</sub> H <sub>6</sub> O <sub>2</sub>	1400.175	2679.107	0.6696	1.4102e-3
glass	2200	910	1.75	-
Copper	8.954e3	380	386	-

**TABLE 4.** various boundary conditions applied over a HCE

Zone	Boundary condition
Inlet	Mass flow rat inlet and fluid inlet temperature
Outlet	Out flow condition
Upper part of absorber tube	No slip condition and heat flux as modeled by S2S and solar load cell
Lower part of absorber tube facing the absorber tube	No slip condition and heat flux (concentrated by mirror reflector)

#### 4. MATHEMATICAL MODELS FOR CALCULATION OF EFFICIENCY OF PARABOLIC SOLAR COLLECTOR

1) Absorbed Flux

$$S = G_T R_b (\alpha\tau)\beta Y \quad (9)$$

2) Convective heat transfer coefficient

$$hf = Nu \times \frac{k}{D_i} \quad (10)$$

where:  $Nu = 0.023 \times Re^{0.8} \times Pr^{0.4}$ ,  $Pr = (\mu \times C_p) / k$ ,  $Re = (\rho \times V \times D_i) / \mu$ ,  $V = (4\dot{m}) / (\pi \times D_i^2 \times \rho)$

3) Useful heat gain

$$qu = \dot{m} C_p (T_{out} - T_{in}) \quad (11)$$

4) Thermal efficiency,  $\eta_t$

$$\eta_t = \frac{\dot{m} c_p (T_{out} - T_{in})}{G_t A_{appert} t} \quad (12)$$

5) Overall efficiency,  $\eta_o$

$$\eta_o = \frac{\dot{m} c_p (T_{out} - T_{in})}{G_{avg} A_{appert}} \quad (13)$$

where,  $G_T$  is global solar intensity in W/m<sup>2</sup>,  $R_b$  is bond resistance,  $\alpha$  is absorptivity of the absorber tube,  $\tau$  is glass cover transmissivity for solar radiation,  $\beta$  is specular reflectivity and  $Y$  is intercept factor,  $N_u$  is

Nusselt number,  $K$  is thermal conductivity in W/m.K,  $D_i$  is inner diameter of absorber tube in m,  $Pr$  is prandtl number,  $\mu$  is dynamic viscosity in Pa.s,  $C_p$  is specific heat in J/kg.K,  $\rho$  is density in kg/m<sup>3</sup>,  $Re$  is reynolds number,  $V$  is average velocity in m/s and  $\dot{m}$  is mass flow rate in kg/sec,  $W$  is width of the solar collector in m,  $L$  is the length of the absorber tube in m,  $A_{appert}$  is the aperture area of the solar collector in m<sup>2</sup>,  $t$  is the time duration and  $G_{avg}$  is the average value of solar radiation in W/m<sup>2</sup>.

## 5 RESULTS

**5. 1. CFD Temperature Contours** CFD temperature contours with different working fluids at different working flow rates of 80LPH are shown in Figures 6(a), 6(b), 6(c), 6(d) and 6(e) for water, 0.05% vol. conc. Al<sub>2</sub>O<sub>3</sub>-C<sub>2</sub>H<sub>6</sub>O<sub>2</sub>-H<sub>2</sub>O, 0.075% vol. conc. Al<sub>2</sub>O<sub>3</sub>-C<sub>2</sub>H<sub>6</sub>O<sub>2</sub>-H<sub>2</sub>O, 0.1% vol. conc. Al<sub>2</sub>O<sub>3</sub>-C<sub>2</sub>H<sub>6</sub>O<sub>2</sub>-H<sub>2</sub>O and 0.125% vol. conc. Al<sub>2</sub>O<sub>3</sub>-C<sub>2</sub>H<sub>6</sub>O<sub>2</sub>-H<sub>2</sub>O. It is seen that maximum temperature rise is achieved when 0.125% vol. conc. Al<sub>2</sub>O<sub>3</sub>-C<sub>2</sub>H<sub>6</sub>O<sub>2</sub>-H<sub>2</sub>O (DI) nanofluid is used as working fluid as compared to other used working fluids.

### 5. 2. Effect of Thermal Efficiency of The Parabolic Solar Collector With Different Working Fluids at Different Mass Flow Rates

Variation of the thermal efficiency both experimental and simulated ones with time of day, for all different working fluids at different mass flow rates of 30 LPH, 50 LPH and 80 LPH are shown in Figures 7,8,9,10,11 and 12. It is seen that both theoretical and simulated values of thermal efficiency are higher for Al<sub>2</sub>O<sub>3</sub>-C<sub>2</sub>H<sub>6</sub>O<sub>2</sub>-H<sub>2</sub>O (DI) working fluid as compared to other different working fluids. Also, nanofluid shows better thermal efficiency as compared to water at most of times. Also, with increasing vol. conc. of nanofluid corresponding improvement in the thermal efficiency of solar collector also takes place.

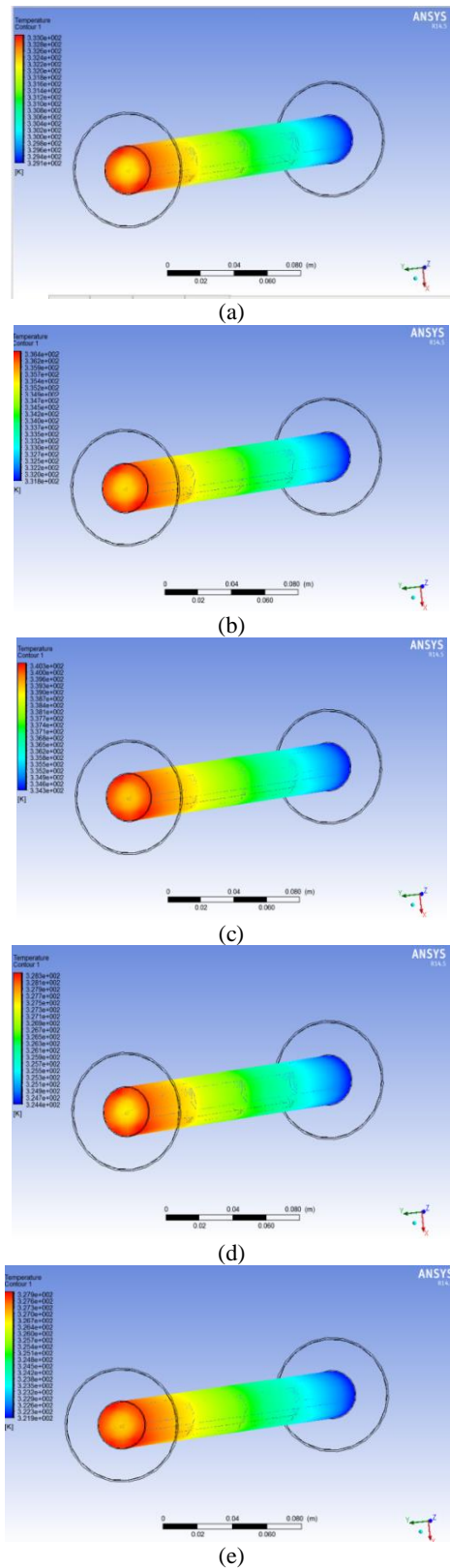


**Figure 6.** temperature contours with different working fluids at 80 LPH (a) H<sub>2</sub>O-C<sub>2</sub>H<sub>6</sub>O<sub>2</sub>, (b) 0.05% vol. conc. Al<sub>2</sub>O<sub>3</sub>-H<sub>2</sub>O-C<sub>2</sub>H<sub>6</sub>O<sub>2</sub>, (c) 0.075% vol. conc. Al<sub>2</sub>O<sub>3</sub>-H<sub>2</sub>O-C<sub>2</sub>H<sub>6</sub>O<sub>2</sub>, (d) 0.1% vol. conc. Al<sub>2</sub>O<sub>3</sub>-H<sub>2</sub>O-C<sub>2</sub>H<sub>6</sub>O<sub>2</sub>, (e) 0.125% vol. conc. Al<sub>2</sub>O<sub>3</sub>-H<sub>2</sub>O-C<sub>2</sub>H<sub>6</sub>O<sub>2</sub>

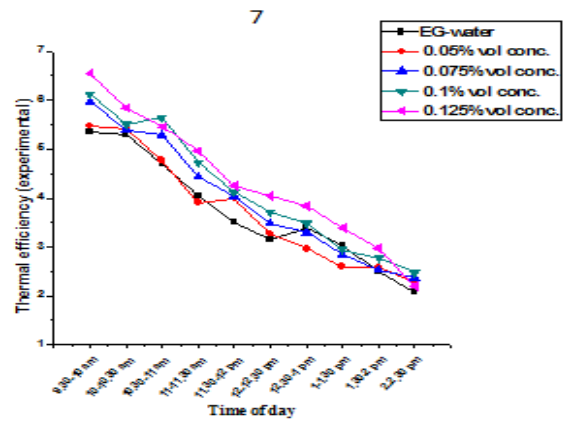


**Figure 7.** Variation of the experimental thermal efficiency with time of day, for all different working fluids at different mass flow rate of 30 LPH

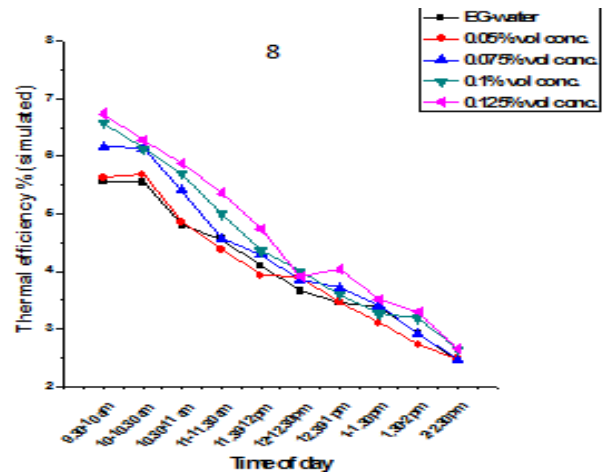


**Figure 8.** Variation of the simulated thermal efficiency with time of day, for all different working fluids at different mass flow rate of 30 LPH

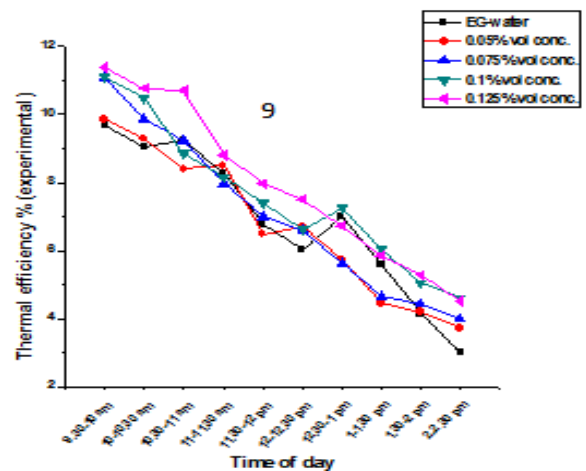


**Figure 9.** Variation of the experimental thermal efficiency with time of day, for all different working fluids at different mass flow rate of 50 LPH

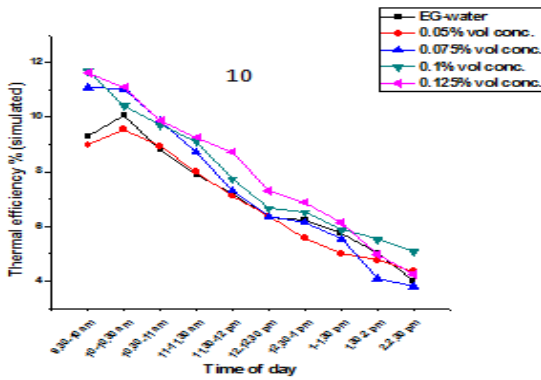


**Figure 10.** Variation of the simulated thermal efficiency with time of day, for all different working fluids at different mass flow rate of 50 LPH

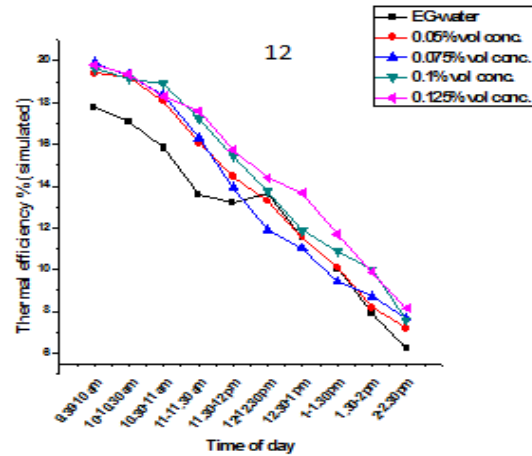
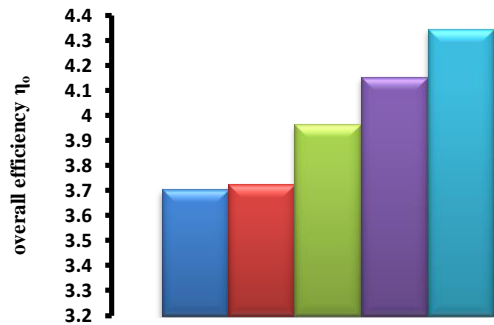


**Figure 12.** Variation of the simulated thermal efficiency with time of day, for all different working fluids at different mass flow rate of 80 LPH

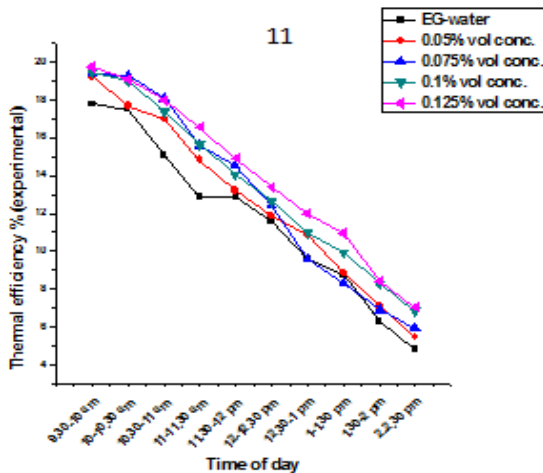
**5. 3. Comparison of Different Working Fluids on the Overall Efficiency of the Parabolic Soar Collector**

Figure 12 shows the comparison of water-ethylene glycol (60:40 v/v) and alumina water-ethylene glycol (60:40 v/v) based nanofluid of different volumetric concentrations at volume flow rate of 30 LPH on collector overall efficiency through both experimental and simulated results respectively. From experimental results it is seen that an improvement of about 4, 7, 12.1 and 14.9% is seen with usage of  $Al_2O_3-C_2H_6O_2-H_2O$  nanofluid. At 50 LPH an improvement of about 2.8, 5.8, 9.8 and 15.8% is seen with usage of  $Al_2O_3-C_2H_6O_2-H_2O$  nanofluid of 0.05, 0.075, 0.1 and 0.125% respectively as compared with water as shown in Figure 13. Figure 14 shows an improvement of about 7.7, 11.3, 15.6 and 16.7% with usage of  $Al_2O_3-C_2H_6O_2-H_2O$  nanofluid of 0.05, 0.075, 0.1 and 0.125% respectively as compared with water.

Legend for Figure 12(a): EG-water (blue), 0.05% vol conc. (red), 0.075% vol conc. (green), 0.1% vol conc. (purple), 0.125% vol conc. (cyan)

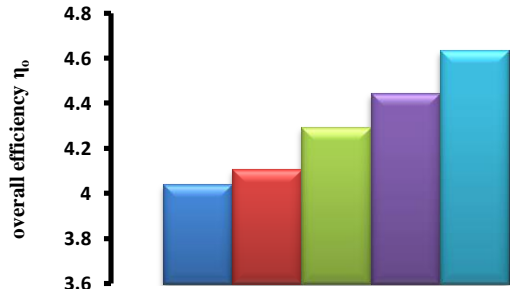


(a)



**Figure 11.** Variation of the experimental thermal efficiency with time of day, for all different working fluids at different mass flow rate of 80 LPH

Legend for Figure 12(b): EG-water (blue), 0.05% vol conc. (red), 0.075% vol conc. (green), 0.1% vol conc. (purple), 0.125% vol conc. (cyan)



(b)

**Figure 12.** Effect of water- ethylene glycol mixture (60:40 v/v) and alumina-water-ethylene glycol mixture (60:40 v/v) based nanofluid as a working fluid on collector’s overall efficiency at 30 LPH (a) Experimental value (b) Simulated value

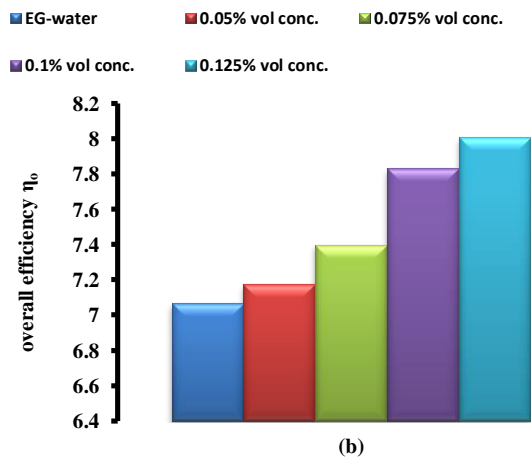
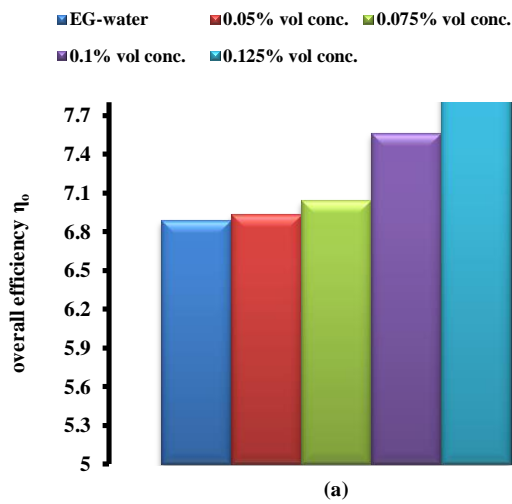


**Figure 13.** Effect of water- ethylene glycol mixture (60:40 v/v) and alumina-water-ethylene glycol mixture (60:40 v/v) based nanofluid as a working fluid on collector’s overall efficiency at 50 LPH (a) Experimental value (b) Simulated value

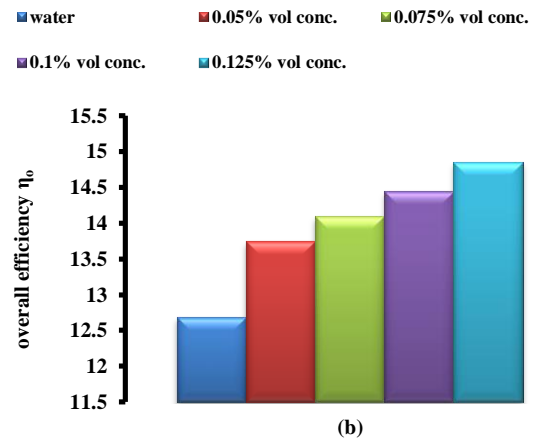
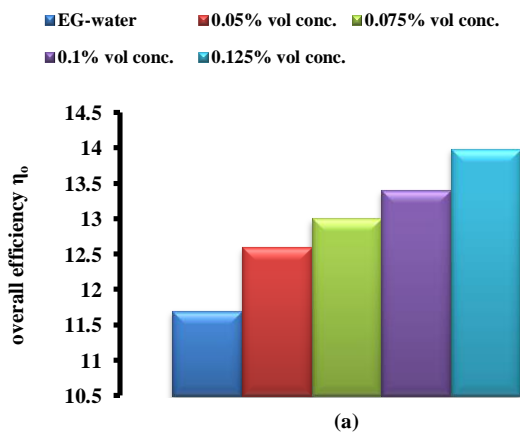


**Figure 14.** Effect of water- ethylene glycol mixture (60:40 v/v) and alumina-water-ethylene glycol mixture (60:40 v/v) based nanofluid as a working fluid on collector’s overall efficiency at 80 LPH (a) Experimental value (b) Simulated value

## 6. CONCLUSIONS

The influence of  $Al_2O_3-C_2H_6O_2-H_2O$  nanofluid on the performance of parabolic solar collector is evaluated using both experimental and CFD analysis. Results of both experimental and CFD shows that improvement in the overall efficiency of solar collector is reported when nanofluid is used as compared to water. Maximum overall efficiency of 14.8% is observed with 0.125% vol. conc.  $Al_2O_3-C_2H_6O_2-H_2O$  (DI) nanofluid at 80 LPH from CFD analysis, while from experimental analysis maximum overall efficiency of about 13.8% is reported. Also, with the increment in the volume flow rate of the working fluid, corresponding enhancement in the collector’s efficiency is witnessed. Improvement of about 17.6% is obtained as the volume flow rate of 0.125% vol. conc.  $Al_2O_3-C_2H_6O_2-H_2O$  (DI) nanofluid is increased from 30 LPH to 80 LPH. Moreover, both experimental and CFD simulated results are in close agreement with a maximum difference of 8.7%.

## 7. REFERENCES

1. Wall, A., "Advantages and disadvantages of solar energy", in *Process Industry Forum*. Vol. 7, (2013), 395-408.
2. Sozen, A., Menlik, T. and Ünvar, S., "Determination of efficiency of flat-plate solar collectors using neural network approach", *Expert Systems with Applications*, Vol. 35, No. 4, (2008), 1533-1539.
3. Zhai, H., Dai, Y., Wu, J., Wang, R. and Zhang, L., "Experimental investigation and analysis on a concentrating solar collector using linear fresnel lens", *Energy Conversion and Management*, Vol. 51, No. 1, (2010), 48-55.
4. Sani, E., Mercatelli, L., Barison, S., Pagura, C., Agresti, F., Colla, L. and Sansoni, P., "Potential of carbon nanohorn-based



- suspensions for solar thermal collectors", *Solar Energy Materials and Solar Cells*, Vol. 95, No. 11, (2011), 2994-3000.
5. Barlev, D., Vidu, R. and Stroeve, P., "Innovation in concentrated solar power", *Solar Energy Materials and Solar Cells*, Vol. 95, No. 10, (2011), 2703-2725.
  6. Philip, J. and Shima, P., "Thermal properties of nanofluids", *Advances in Colloid and Interface Science*, Vol. 183, (2012), 30-45.
  7. Wong, K.V. and De Leon, O., "Applications of nanofluids: Current and future", *Advances in Mechanical Engineering*, Vol. 2, (2010), 1-11.
  8. Lee, S., Choi, S.-S., Li, S., and Eastman, J., "Measuring thermal conductivity of fluids containing oxide nanoparticles", *Journal of Heat transfer*, Vol. 121, No. 2, (1999), 280-289.
  9. Khullar, V. and Tyagi, H., "A study on environmental impact of nanofluid-based concentrating solar water heating system", *International Journal of Environmental Studies*, Vol. 69, No. 2, (2012), 220-232.
  10. Tyagi, H., Phelan, P. and Prasher, R., "Predicted efficiency of a low-temperature nanofluid-based direct absorption solar collector", *Journal of Solar Energy Engineering*, Vol. 131, No. 4, (2009), 1-7.
  11. Otanicar, T.P., Phelan, P.E., Prasher, R.S., Rosengarten, G. and Taylor, R.A., "Nanofluid-based direct absorption solar collector", *Journal of Renewable and Sustainable Energy*, Vol. 2, No. 3, (2010), 1-13.
  12. Chougule, S.S., Pise, A.T. and Madane, P.A., "Performance of nanofluid-charged solar water heater by solar tracking system", in *Advances in Engineering, Science and Management (ICAESM), International Conference on, IEEE.*, (2012), 247-253.
  13. Han, D., Meng, Z., Wu, D., Zhang, C. and Zhu, H., "Thermal properties of carbon black aqueous nanofluids for solar absorption", *Nanoscale Research Letters*, Vol. 6, No. 1, (2011), 1-7.
  14. Chaji, H., Ajabshirchi, Y., Esmaeilzadeh, E., Heris, S.Z., Hedayatzadeh, M. and Kahani, M., "Experimental study on thermal efficiency of flat plate solar collector using  $\text{TiO}_2$  / water nanofluid", *Modern Applied Science*, Vol. 7, No. 10, (2013), 60-69.
  15. Alim, M., Abdin, Z., Saidur, R., Hepbasli, A., Khairul, M. and Rahim, N., "Analyses of entropy generation and pressure drop for a conventional flat plate solar collector using different types of metal oxide nanofluids", *Energy and Buildings*, Vol. 66, (2013), 289-296.

## Performance Evaluation of Nanofluid ( $\text{Al}_2\text{O}_3/\text{H}_2\text{O}-\text{C}_2\text{H}_6\text{O}_2$ ) Based Parabolic Solar Collector Using Both Experimental and CFD Techniques

K. Ajay, L. Kundan

Mechanical Engineering Department, Thapar University, India

### PAPER INFO

چکیده

#### Paper history:

Received 04 December 2015

Received in revised form 20 February 2016

Accepted 14 April 2016

#### Keywords:

Solar Energy

Parabolic Solar Collector

CFD

Nanofluid

Thermal Efficiency

کار حاضر، عملکرد کلکتور خورشیدی را با استفاده از نانوسیال  $\text{Al}_2\text{O}_3-\text{C}_2\text{H}_6\text{O}_2-\text{H}_2\text{O}$  به عنوان سیال کاری از طریق هم تجزیه و تحلیل تجربی و هم CFD ارزیابی می کند. مخلوط اتیلن گلیکول-آب (۶۰:۴۰ V/V) به عنوان سیال پایه، که در آن نانوذرات  $\alpha-\text{Al}_2\text{O}_3$  به اندازه متوسط ۲۰ نانومتر برای آماده سازی نانو سیال با چهار غلظت مختلف حجمی ۰/۰۵، ۰/۰۷۵، ۰/۱ و ۰/۱۲۵٪ پراکنده است، استفاده می شود. سه نرخ جریان حجمی مختلف ۳۰ LPH، ۵۰ LPH و ۸۰ LPH استفاده شده است. تجزیه و تحلیل CFD از طریق ANSYS FLUENT 14.5 انجام شده است. از هر دو تجزیه و تحلیل تجربی و CFD، بهبود در بازده کلی کلکتور خورشیدی هنگامی گزارش شده است که از نانو سیال در مقایسه با مخلوط آب-اتیلن گلیکول استفاده شده است. با غلظت حجمی ۰/۱۲۵ درصدی نانو سیال  $\text{Al}_2\text{O}_3-\text{C}_2\text{H}_6\text{O}_2-\text{H}_2\text{O}$  (DI)، حداکثر بازده کلی حدود ۴/۶، ۷/۹ و ۱۴/۸٪ به ترتیب در ۳۰ LPH، ۵۰ LPH و ۸۰ LPH با استفاده از نتایج CFD گزارش شده است، در حالی که از نتایج تجربی حداکثر بازده کلی حدود ۴/۳، ۷/۵ و ۱۳/۸٪ به ترتیب در ۳۰ LPH، ۵۰ LPH و ۸۰ LPH دیده می شود. همچنین، با افزایش میزان جریان حجمی سیال کاری، بهبود در بازده کلی کلکتور خورشیدی رخ می دهد. تطابق نزدیکی نیز بین نتیجه CFD و تجربی توسعه یافته است.

doi: 10.5829/idosi.ije.2016.29.04a.17